Homogeneity vs. Heterogeneity of Porosity in Boom Clay

Susanne Hemes[1*], Guillaume Desbois[1], Janos L. Urai[1], Mieke De Craen[2], Miroslav Honty [2]

[1] Structural geology, Tectonics and Geomechanics, RWTH Aachen University (Germany)
[2] SCK-CEN, Belgian Nuclear Research Centre (Belgium)

* s.hemes@ged.rwth-aachen.de

Abstract

Microstructural investigations on Boom Clay at nano- to micrometer scale, using BIB-SEM methods, result in porosity characterization for different mineral phases from direct observations on high resolution SE2-images of representative elementary areas (REAs).
High quality, polished surfaces of cross-sections of ~ 1 mm^2 size were produced on three different samples from the Mol-Dessel research site (Belgium). More than 33,000 pores were detected, manually segmented and analyzed with regard to their size, shape and orientation. Two main pore classes were defined: Small pores (< 500 nm (ED)) within the clay matrices of samples and 'big' pores (> 500 nm (ED)) at the interfaces between clay and non-clay mineral (NCM) grains. Samples investigated show similar porosities regarding the first pore-class, but differences occur at the interfaces between clay matrix and NCM grains. These differences were interpreted to be due to differences in quantitative mineralogy (amount of non-clay mineral grains) and grain-size distributions between samples investigated. Visible porosities were measured as 15 to 17 % for samples investigated. Pore-size distributions of pores in clay are similar for all samples, showing log-normal distributions with peaks around 60 nm (ED) and more than 95 % of the pores being smaller than 500 nm (ED). Fitting pore-size distributions using power-laws with exponents between 1.56 and 1.7, assuming self-similarity of the pore space, thus pores smaller than the pore detection resolution following the same power-laws and using these power-laws for extrapolation of pore-size distributions below the limit of pore detection resolution, results in total estimated porosities between 20 and 30 %. These results are in good agreement with data known from Mercury Porosimetry investigations (35-40 % porosity) and water content porosity measurements (~ 36 %) performed on Boom Clay (Boisson, 2005).

Introduction

The aim of this study is to characterize and quantify the vertical variability of Boom Clay porosity on a nano- to micrometer scale, using Broad Ion Beam (BIB) – Scanning Electron Microscopy (SEM) method. All samples investigated in this study are from the Mol1-borehole and part of the EZE sample series. Samples were chosen due to end-member mineralogical compositions and grain-size distributions within the Mol1-borehole/EZE sample series. Sample 1 (EZE55) is from the level of the HADES-research laboratory (~ 225 meters depth) and of an intermediate mineralogical composition (~ 50 wt % clay) as well as grain-size distribution. Sample 2 (EZE52) is a very coarse-grained example of Boom Clay and very poor in clay minerals (only ~ 34 wt %). It originates from a lower depth of the

Mol1-borehole (~ 197 meters). Sample 3 (EZE54) is the most fine-grained and clay-rich (~ 60 wt % clay) sample investigated in this study and from ~ 214 meters depth.

Method

Samples were received pre-dried, in cores of ~ 10 cm diameter. After cutting into smaller pieces of ~ 1 x 0.5 x 0.3 cm size using a razorblade, samples were dried in an oven at 60°C for 72 hours. Afterwards samples were pre-polished using carbide-sandpapers of several grain-sizes to improve the quality of the BIB-milling. BIB polishing was performed for 7.45 hours at 6 kV using a stand alone 'JEOL SM-09010' BIB-polisher. High quality polished cross-sections of ~ 1 mm^2 size were produced for high resolution SEM-imaging. Before SEM-imaging samples were coated with a thin layer of gold to prevent them from charging. SEM-imaging was performed on a 'ZEISS, supra 55'. To be able to investigate porosities in REAs and at pore-scale, hundreds of high resolution single SE2-images were taken as mosaics and stitched together afterwards automatically using 'Autopano'. Pore detection and segmentation was done according to grey-values of SE2-images, either manually in ArcGIS or automatically using a combined 'thresholding-sobel edge detection' approach in Matlab. Pore-sizes, shapes and orientations were calculated and analyzed in ArcGIS, Matlab (toolbox PolyLX, Lexa et al., 2005) and Microsoft Excel.

Results

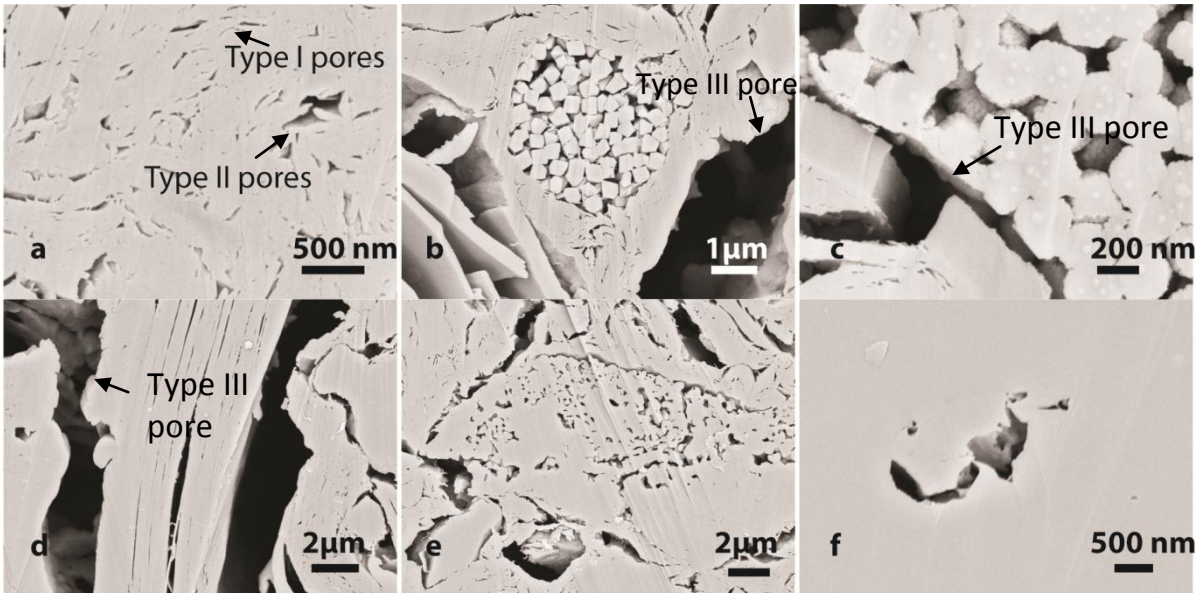

Figure 1. Pore morphologies in different mineral phases (a: Clay, Type I and Type II pores as described in Desbois et al., 2009, b+c: Pyrite, d: Mica, e: Fossil, f: Quartz).

More than 33,000 pores were detected and outlined manually. Characteristic pore morphologies were found for each mineral phase, present in the investigated samples. Similarities were found for pores within the clay matrices of samples investigated, regardless of the samples' origin, mineralogical composition and grain-size distribution. Pores within clay are as described in Desbois et al., 2009 (Figure 1a, type I and type II pores). Most (> 95 %) of them are smaller than 500 nm (ED) with prevailing orientations parallel to the bedding of samples. Much bigger – up to 2 µm (ED) in the two finer

grained samples and up to 20 µm (ED) in the coarse-grained sample, mostly elongated – pores with long-axis orientations sub-parallel to the grain boundaries or of triangular shape with no preferred orientations, were found at the clay-NCM interfaces (type III pores, Desbois, 2009).
Pores in pyrite framboids are usually < 500 nm (ED) and of shapes controlled by the pyrite single grains' arrangement (Figure 1b and c). Pores in mica are elongated with very high aspect ratios and short axis typically < 200 nm (Figure 1d). Pores inside fossils show rounded edges and are typically smaller than 500 nm (ED) (Figure 1e). Pores inside quartz and feldspar grains occur only in very few amounts and are usually < 500 nm (ED) (Figure 1f).

Pore-size distributions were calculated for pores within the clay matrices of samples (Figure 2). More than 95 % of the pores within the clay matrices are smaller than 500 nm (ED), but whereas in the two finer grained samples no pores > 2 µm (ED) have been detected, in the coarse-grained sample pores up to an equivalent diameter of ~ 20 µm were found. Pore-sizes in the clay matrices are log-normally distributed with peaks around 60 nm (ED) in all samples investigated.

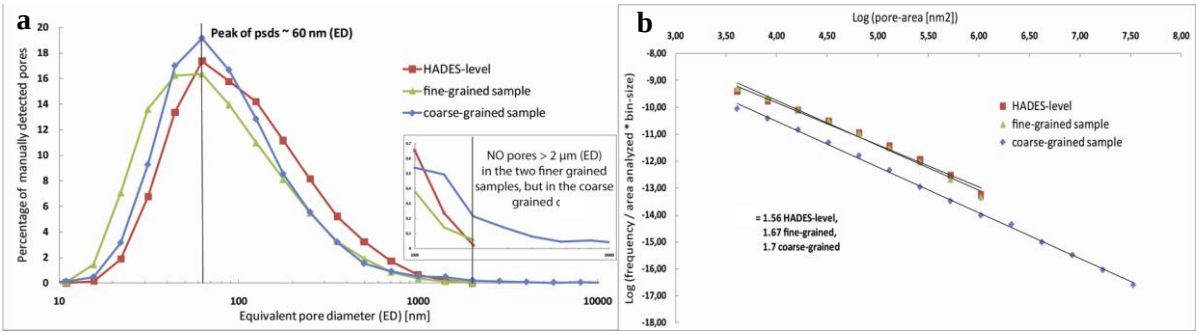

Figure 2. Pore-size distributions of visible pores measured within the clay matrices of samples; b: Power-law fitting of psds with power-law exponents between 1.56 and 1.7.

Total visible porosities were measured as 16.4 % for the HADES-level sample, 16.5 % for the coarse-grained sample and 15.2 % for the fine-grained sample. In the two finer grained samples pores > 500 nm (ED), which mostly occur at the clay-NCM interfaces account for ~ 50 % of the total visible porosity, whereas in the coarse-grained sample these big pores close to NCM grains account for ~ 80 % of the total visible porosity.
Power-laws were used to fit pore-size distributions, with power-law exponents between 1.56 and 1.7. Pore-size distributions were extrapolated below the pore detection resolution (pdr) (~ 50-60 nm (ED)) down to equivalent pore diameters of 1 nm, using these power-laws. Extrapolation of pore-size distributions results in total estimated porosities of 20 % for the coarse-grained sample, 24 % for the fine-grained sample and 30 % for the HADES-level sample.

Discussion and Conclusions

Pore morphologies within the clay matrices of samples investigated are similar, irrespective of the samples' origin, mineralogical composition or grain-size distribution. Differences occur at the interface between clay and NCM-grains: Pore-sizes depend on the grain-size of the sample. Differences in total observed porosities between samples investigated are interpreted to be due to differences in mineralogical composition (NCM-content) and grain-size distribution of samples.
Visible porosities of 15-17 % from BIB-SEM investigations in a pore-size range between ~ 50 nm (pdr) and 2,000/20,000 nm (ED) (largest pores found in REAs investigated) are lower than expected for Boom Clay (e.g. from Mercury Porosimetry injection: 35-40 % or water content porosity measurements: ~ 36 %, Boisson, 2005).

However, estimated porosities from extrapolation of pore-size distributions below the limit of pdr, assuming self-similarity of the pore space, are in the range of values expected and measured for connected porosities in BC. This leads to the conclusion that connecting pore throats in Boom Clay are smaller than 10-50 nm (pore throat diameter), since no interconnected pores were observed at the scale of resolution.

The presented method delivers a mean to visualize, characterize and quantify porosity of argillaceous materials in REAs down to the nm-resolution. It has been shown that up-scaling from microstructural investigations at pore-scale to bulk sample properties is possible, making some general assumptions.

Acknowledgement

Thanks to ONDRAF/NIRAS and SCK/CEN for funding and support.

References

Boisson, J.Y. (2005) Clay Club Catalogue of Characteristics of Argillaceous Rocks, OECD/NEA/RWMC/IGSC (Working Group on Measurement and Physical Understanding of Groundwater Flow through Argillaceous Media). *Report NEA No. **4436.** OECD/NEA Paris, France (p. 72).*

Desbois, G., Urai, J.L. and Kukla, P.A. (2009) Morphology of the pore space in claystones – evidence from BIB/FIB ion beam sectioning and cryo-SEM observations. *e-Earth **4***, 1-8/15-22.

Lexa, O., Štípská, P., Schulmann, K., Baratoux, L. and Kröner, A. (2005) Contrasting textural

record of two distinct metamorphic events of similar P-T conditions and different durations. *Journal of Metamorphic Geology **23 (8)***, 649–666.